Electronic Supplementary Information for

Fabrication of Superior-Performance SnO$_2$@C Composites for Lithium-Ion Anodes Using Tubular Mesoporous Carbons with Thin Carbon Wall and High Pore Volume

Fei Han,[a] Wen-Cui Li,[a] Ming-Run Li,[b] and An-Hui Lu*[a]

[a]State Key Laboratory of Fine Chemicals, School of Chemical Engineering, Faculty of Chemical, Environmental and Biological Science and Technology, Dalian University of Technology, Dalian 116024, P. R. China
[b]State Key Laboratory of Catalysis, Dalian Institute of Chemical Physics, Chinese Academy of Sciences, Dalian 116023, P. R. China

*E-mail: anhuilu@dlut.edu.cn, Tel/Fax: +86-411-84986112
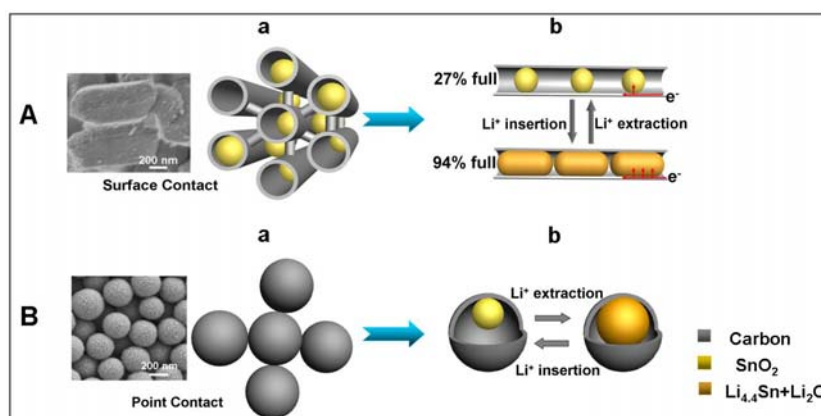
Scheme S1. Schematic illustration for particle contact areas (a), and particle size changes during Li$^+$ insertion/extraction processes (b). (A) Rod-like meosporous carbon granules in our study, and (B) Spherical core-shell SnO$_2$@C nanostructures in the literature. Judging from A and B, one can easily envisage that the electrical conductivity of the close packed rod granules (large surface contact area) is superior to that of the close packed spheres (point contact). Especially during a charge process, the contact pattern is still point contact between the core and the shell. Differently, expansion of SnO$_2$ NPs along the tubular channels results in an increased contact area between SnO$_2$ NPs and the thin carbon walls.
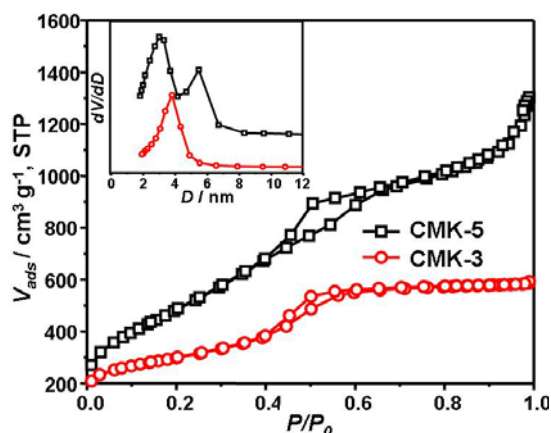
Fig. S1 N_2 sorption isotherms and pore size distributions (inset) of CMK-5 and CMK-3.

Computational Modeling of Filling Degree:

To calculate the filling degree of pore channels before and after Li^+ insertion, we follow a simple model for the composite with different matrixs and SnO_2 loadings. On the basis of the specific pore volume of carbon matrixs (2.16 $cm^3 \ g^{-1}$ of CMK-5 and 0.92 $cm^3 \ g^{-1}$ of CMK-3) and the density of bulk SnO_2 (6.95 $g \ cm^{-3}$, from Lange's Handbook of Chemistry), the filling degree of a composite is calculated by equation:

$$\varphi_{filling \ degree} = \frac{\omega_{SnO_2} / \rho_{SnO_2}}{\omega_{carbon} \times V_{carbon}}$$

Here, φ is the filling degree; ω represents the content of different component; ρ indicates the density and V is the pore volume.

The volume expansion factor of SnO_2 after Li^+ insertion is ca. 3.5,[1] indicating the filling degree of $Li_{4.4}Sn$ is 3.5 times of the original filling degree. Hence, it is necessary for a considerably large void space to compensate for the huge volume expansion of SnO_2 NPs.
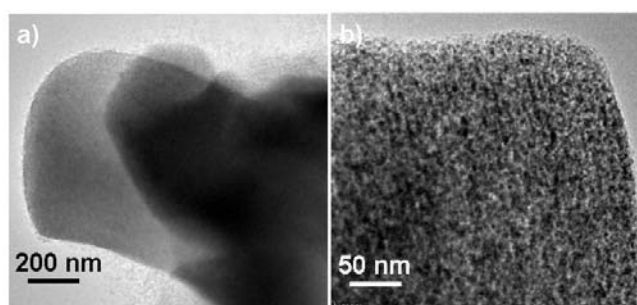

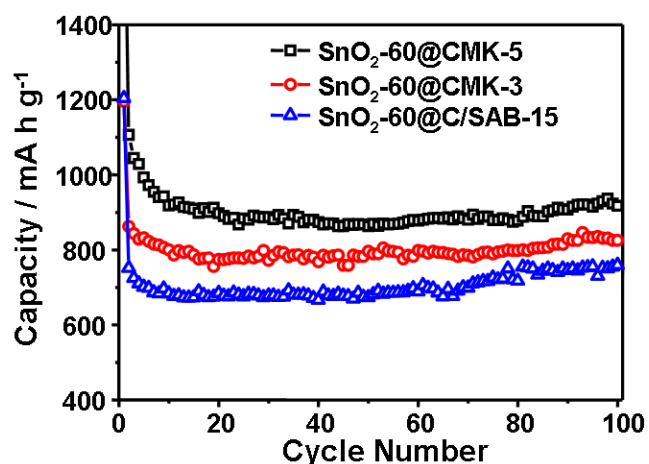Fig. S2 TEM images of SnO_2-60@CMK-5.

Fig. S3 Cycle performance of composites at a current density of 200 mA g^{-1} between 0.005 and 3 V, by taking the carbon mass of $SnO_2@C$ into account.

The sample SnO_2-60@C/SBA-15 with ~60 wt % SnO_2 loading was prepared by using C/SBA-15 composite as the template for the encapsulation of SnO_2 nanoparticles, followed by etching out the silica to reserve a vacant small pore channel (3 nm). A comparison of cycle performance of three $SnO_2@C$ composites based on different carbon matrix is presented in Fig. S3. Remarkably, the reversible capacity of SnO_2-60@C/SBA-15 is lowest in those three $SnO_2@C$ composite. Therefore, we focus on using CMK-5 as the carbon matrix in the following up study.

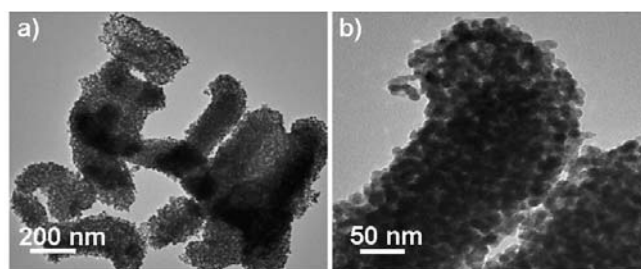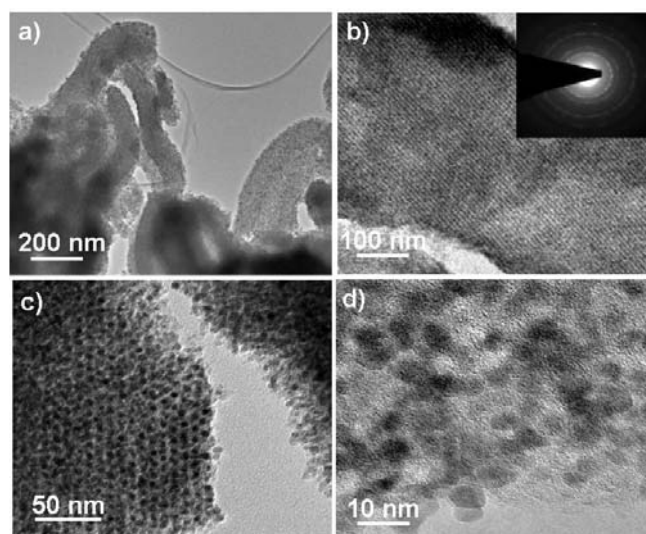Fig. S4 TEM images of Nanocast SnO_2.

3

Fig. S5 TEM images of SnO_2-80@CMK-5 (inset: SAED pattern).

Table S1. Comparison of the electrochemical data of SnO_2@C composites from literature.

Type of material	Current density (mA g^{-1})	Voltage range (V)	Initial efficiency (%)	Cycles	Reversible capacity after cycles (mA h g^{-1})	Reference
SnO_2@CMK-5 tubular composite	200	0.005-3	71	100	1039	This study
Ordered SnO_2/CMK-3 nanocomposites	100	0.01-2	36	35	546	2
SnO_2/Graphene nanoporous materials	50	0.05-2	43	30	570	3
Coaxial SnO_2@carbon hollow nanospheres	200	0.005-2	41	100	510	4
SnO_2-CNT composite sheet	40	0.01-3	61	56	985	5
SnO_2-tube-in-CNT nanostructure	340	0.005-3	53	200	542	6
Mesoporous SnO_2 on MWCNTs	33.3	0.005-2	74	50	345	7
Core-shell SnO_2@C composites	100	0.005-2	67	50	630	8
SnO_2/Fc@SWNTs composite	150	0.05-3	60	40	905	9
C@SnO_2 core-sheath composite	50	0.005-2.8	69	100	540	10
SnO_2@C hollow spheres	100	0.005-2	45	50	473	11
CNTs@SnO_2@C coaxial nanocables	100	0.01-2	49	65	463	12
SnO_2 nanorods@graphene sheets	200	0.005-3	66	50	575	13

Computational Modeling for Capacity:

In order to clarify the influence of the CMK-5 matrix for SnO_2 NPs on the electrochemical performance of SnO_2@CMK-5 composites, we have calculated the practical capacity of SnO_2 NPs from the total average capacity of SnO_2-80@CMK-5 (1000 mA h g^{-1}) and CMK-5 (470 mA h g^{-1}). The calculated capacity of a physical mixture with 20 wt % of CMK-5 and 80 wt % of SnO_2 was based on the following equation:

$C_{SnO2} = (C_{total} - C_{CMK-5} \times \omega_{CMK-5}) / \omega_{SnO2} = (1000 - 470 \times 0.2) / 0.8 = 1133$ mA h g^{-1}

To support this approach, the theoretical capacity of another composite SnO_2-60@CMK-5 was estimated from the practical capacity of SnO_2 (1133 mA h g^{-1}) following the below equation:

$C_{theoretical} = C_{SnO2} \times \omega_{SnO2} + C_{CMK-5} \times \omega_{CMK-5} = 1133 \times 0.6 + 470 \times 0.4 = 868$ mA h g^{-1}

Indeed, the observed capacity (890 mA h g^{-1}) of the SnO_2-60@CMK-5 composite is similar to the theoretical capacity, highlighting the superior performance of SnO_2@CMK-5 composites as LIBs anodes.
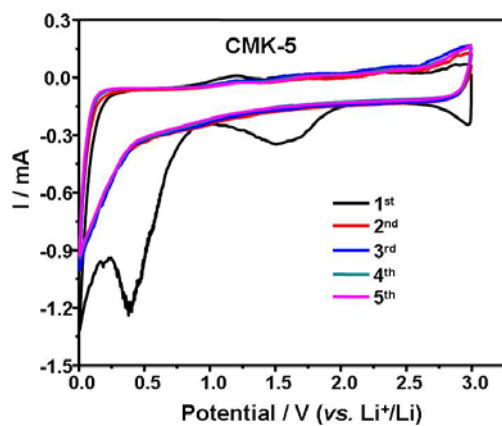
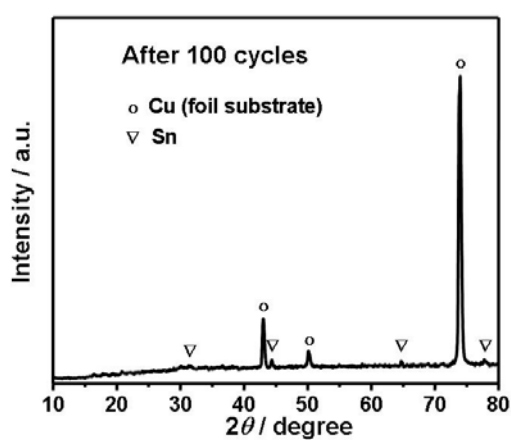Fig. S6 Cyclic voltammograms of pure CMK-5 anode at a scan rate of 0.2 mV s^{-1}.

Fig. S7 XRD pattern of SnO$_2$-80@CMK-5 anode after 100 cycles. The strong peaks are assigned to metallic Cu from a Cu foil substrate used in battery test.
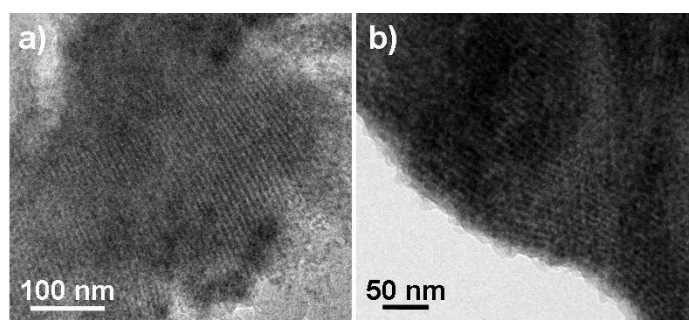

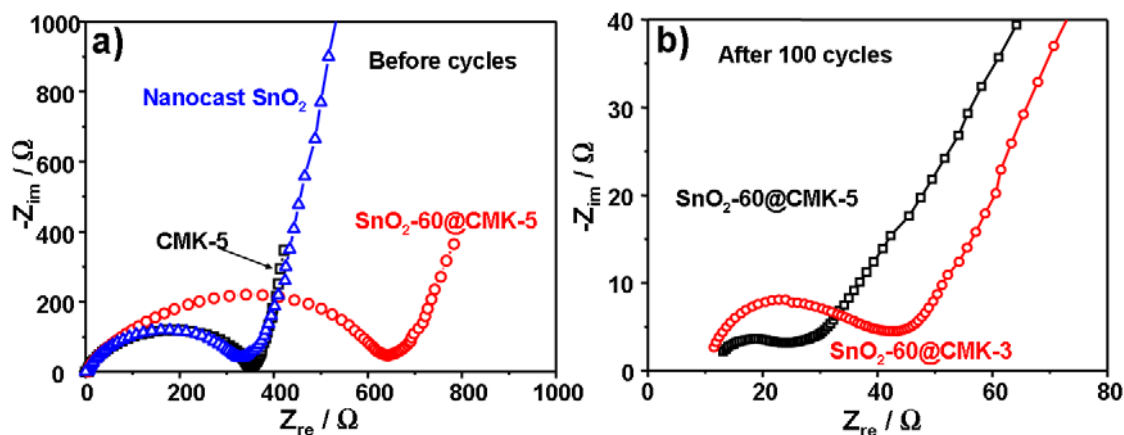Fig. S8 TEM images of SnO$_2$-80@CMK-5 after 100 cycles

Fig. S9 Electrochemical impedance spectra obtained by applying a sine wave with amplitude of 5.0 mV over a frequency range 100 kHz–0.01 Hz.

As shown as in Fig. S9a, the charge transfer resistances of CMK-5 and nanocast SnO_2 are almost equivalent and less than that of SnO_2-60@CMK-5. Meanwhile, Fig. S9b reveals that after 100 cycles the conductivity of SnO_2-60@CMK-5 is better than that of SnO_2-60@CMK-3, indicating that tubular mesoporous carbon CMK-5 with thin carbon walls and high pore volume is more suitable than CMK-3 with thick carbon walls and low pore volume for loading SnO_2 as the anodes.

References

1   J. Y. Huang, L. Zhong, C. M. Wang, J. P. Sullivan, W. Xu, L. Q. Zhang, S. X. Mao, N. S. Hudak, X. H. Liu, A. Subramanian, H. Fan, L. Qi, A. Kushima and J. Li, *Science*, 2010, **330**, 1515.
2   H. Qiao, J. Li, J. Fu, D. Kumar, Q. Wei, Y. Cai and F. Huang, *ACS Appl. Mater. Interfaces*, 2011, **3**, 3704.
3   S.-M. Paek, E. Yoo and I. Honma, *Nano Lett.*, 2009, **9**, 72.
4   X. W. Lou, C. M. Li and L. A. Archer, *Adv. Mater.*, 2009, **21**, 2536.
5   H.-X. Zhang, C. Feng, Y.-C. Zhai, K.-L. Jiang, Q.-Q. Li and S.-S. Fan, *Adv. Mater.*, 2009, **21**, 2299.
6   Y. Wang, H. C. Zeng and J. Y. Lee, *Adv. Mater.*, 2006, **18**, 645.
7   Z. Wen, Q. Wang, Q. Zhang and J. Li, *Adv. Funct. Mater.*, 2007, **17**, 2772.
8   J. Liu, W. Li and A. Manthiram, *Chem. Commun.*, 2010, **46**, 1437.
9   J. Li, Y. Zhao, N. Wang and L. Guan, *Chem. Commun.*, 2011, **47**, 5238.
10 L. Ji, Z. Lin, B. Guo, A. J. Medford and X. Zhang, *Chem. Eur. J.*, 2010, **16**, 11543.
11 X. W. Lou, D. Deng, J. Y. Lee and L. A. Archer, *Chem. Mater.*, 2008, **20**, 6562.
12 P. Wu, N. Du, H. Zhang, J. Yu and D. Yang, *J. Phys. Chem. C*, 2010, **114**, 22535.
13 C. Xu, J. Sun and L. Gao, *J. Mater. Chem.*, 2012, **22**, 975.